

Optimal band gap for improved thermoelectric performance of two-dimensional Dirac materials

Eddwi H. Hasdeo,^{1,*} Lukas P. A. Krisna,² Bobby E. Gunara,² Nguyen T. Hung,³ and Ahmad. R. T. Nugraha^{1,3,†}

¹*Research Center for Physics, Indonesian Institute of Sciences (LIPI), Tangerang Selatan 15314, Indonesia*

²*Theoretical High Energy Physics and Instrumentation Research Group,
Faculty of Mathematics and Natural Sciences, Institut Teknologi Bandung, Bandung 40132, Indonesia*

³*Department of Physics, Tohoku University, Sendai 980-8578, Japan*

(Dated: December 15, 2024)

Thermoelectric properties of two-dimensional (2D) Dirac materials are calculated within linearized Boltzmann transport theory and relaxation time approximation. We find that the gapless 2D Dirac material exhibits poorer thermoelectric performance than the gapped one. Furthermore, there exists an optimal band gap for maximizing figure of merit (ZT) in the gapped 2D Dirac material. The optimal band gap ranges from $6k_B T$ to $18k_B T$, where k_B is the Boltzmann constant and T is the operating temperature in kelvin. This result, which is similar to that for bulk semiconductors, indicates the importance of having narrow gaps to achieve the best thermoelectrics in 2D systems. Larger maximum ZT s can also be obtained by suppressing the lattice thermal conductivity. In the most ideal case where the lattice thermal conductivity is zero (leaving the electron thermal conductivity alone), the maximum ZT in the gapped 2D Dirac material is many times ZT of commercial thermoelectric materials.

I. INTRODUCTION

Thermoelectric (TE) materials convert temperature gradient into electricity and thus they are useful for various devices utilizing refrigerators and power generators [1, 2]. However, it is also well recognized that the efficiency of most of TE materials is lower than other energy conversion systems so their applications are still limited in the areas where the efficiency is not an important issue. To expand the applicability of thermoelectrics, there has been extensive studies suggesting different strategies with particular emphasis on improving the efficiency, such as the energy band convergence [3], the hierarchical architecturing [4], and the low-dimensional materials [5, 6]. Theoretically, an efficient TE material should be a good electronic conductor as well as a good thermal insulator. The efficiency of converting heat into electricity is related to the so-called TE figure of merit, $ZT = S^2 \sigma T / \kappa$, where S , σ , κ and T are the Seebeck coefficient, electrical conductivity, thermal conductivity, and operating temperature, respectively. For many decades, it has been a challenging issue even just to find materials with $ZT \approx 1$ since S , σ and κ are generally interrelated [7, 8]. In other words, it is difficult to obtain a TE material with simultaneously large S , large σ , and small κ to maximize ZT [9–11].

Of different strategies to obtain better ZT , miniaturization of materials has been an important route to enhance TE performance, thanks to the quantum confinement effect that modifies the band structure, effective mass, and density of states [5, 6, 12, 13]. Two-dimensional (2D) materials, in particular, are often sug-

gested to have better TE performance than bulk materials [14, 15]. For example, a large power factor, $S^2 \sigma$ (part of the numerator of ZT), has been either theoretically proposed or experimentally observed in various classes of 2D materials such as MoS₂ [16], SnS₂ [17], InSe [18], and some graphene-like materials [19]. Furthermore, by band gap engineering, these 2D materials possess various values of the band gaps, ranging from nearly zero to about 2 eV [20–23], so we may have a lot of choices of materials depending on the purpose. However, the ZT of 2D materials overall remains hard to push above unity. In particular, for the 2D materials with moderate or wide band gaps, the predicted or observed ZT values are mostly less than one [16–18], while the 2D materials with smaller gaps tend to exhibit larger ZT [24]. This tendency reminds us to some of the early works regarding the effect of band gap on the ZT [9, 11], in which it was suggested that the best thermoelectrics in bulk (3D) systems can be obtained with materials having narrow gaps [11, 25]. Motivated by those works, we are wondering if there also exists an optimal gap (or a possible range of optimal gaps) for the 2D materials in order to achieve the best thermoelectrics, which can guide experimentalists to search for 2D materials with high TE performance.

In this work, we focus our attention to the 2D materials whose electronic structure can be modeled by the Dirac Hamiltonian, or the so-called 2D Dirac materials. In fact, most of monolayer 2D materials having excellent electron transport properties can be considered as the 2D Dirac materials, thanks to presence of nonparabolic bands with linear energy dispersion around the Dirac point for the gapless case. As we will show later, the excellent electron transport properties in these materials do not automatically lead to efficient and high-performance thermoelectrics. However, we can maximize the ZT for the 2D Dirac materials by considering the optimal gap. From the calculations of the Seebeck coefficient, electrical con-

* eddw001@lipi.go.id

† art.nugraha@gmail.com

ductivity, thermal conductivity, and thus ZT within linearized Boltzmann transport theory and relaxation time approximation (RTA), we find that the optimal gaps for the 2D Dirac materials are about $6\text{--}18k_B T$. This result is similar with the case of bulk semiconductors whose optimal gaps for the maximal ZT are about $6\text{--}10k_B T$ (the upper limit may be larger depending on the dominant scattering mechanism) [11]. Therefore, although recent trend in TE research utilize moderate-gap or wide-gap 2D semiconductors as potential TE materials [16–18], we would suggest that it is better to use materials with narrow band gaps within $6\text{--}18k_B T$ and then, if needed, we may further enhance their TE performance by other techniques such as doping [26], strain engineering [27], and manufacturing grain boundary or point defect [28] to diminish the phonon thermal conductivity.

II. MODEL AND METHODS

For simplicity, we assume that the energy bands of gapless and gapped Dirac materials are symmetric with respect to $E = 0$. The 2D Dirac material with a band gap $E_g = 2\Delta$ can be described by energy dispersion,

$$E(k) = \pm \sqrt{(\hbar v_g |\mathbf{k}|)^2 + \Delta^2}, \quad (1)$$

where \hbar is the Planck constant, v_g is the group velocity, and \mathbf{k} is the 2D wave vector with magnitude $k = |\mathbf{k}| = \sqrt{k_x^2 + k_y^2}$. This energy dispersion is illustrated in Figs. 1(a) and (b) for gapless ($\Delta = 0$) and gapped (finite Δ) 2D Dirac materials, respectively.

We use the Boltzmann transport theory in the linear response regime and apply the relaxation time approximation (RTA) for an isotropic system, which is valid for our simplified model of 2D Dirac materials whose transport properties do not depend on a particular orientation in the 2D plane. Within this approach, thermoelectric properties of a 2D Dirac material with electronic energy dispersion can be calculated from the transport coefficients

$$\mathcal{L}_i = \int_{-\infty}^{\infty} \mathcal{T}(E) (E - \mu)^i \left(-\frac{\partial f}{\partial E} \right) dE, \quad (2)$$

where μ is the chemical potential (or Fermi energy), $f(E)$ is the Fermi-Dirac distribution, and $\mathcal{T}(E)$ is the transport distribution function (TDF). In Eq. (2), i takes a value of 0, 1, or 2 depending on the thermoelectric properties to be calculated.

The explicit form of TDF is

$$\mathcal{T}(E) = v^2(E) \tau(E) \mathcal{D}(E), \quad (3)$$

where v is the longitudinal velocity in a particular direction, τ is the relaxation time, and $\mathcal{D}(E)$ is the density of states (DOS). Due to the isotropic nature of the 2D

Dirac materials in our model, v can be related with v_g by the following formula:

$$v^2 = \frac{v_g^2}{2} \left(\frac{E^2 - \Delta^2}{E^2} \right). \quad (4)$$

For the energy-dependent relaxation time, we assume that short-ranged impurity scattering dominates the relaxation mechanism and as result the relaxation time is inversely proportional to the DOS [29, 30], i.e.,

$$\tau(E) = C [\mathcal{D}(E)]^{-1}, \quad (5)$$

where C is the scattering coefficient in units of $\text{W}^{-1} \text{m}^{-3}$. This assumption can be derived from Fermi's golden rule and is suitable for the scattering mechanism involving electron-phonon interactions where either acoustic or optical phonons scattered by electrons within temperature range 300–700 K [29–31]. For the sake of completeness, in Appendix we also present the calculation result within a less accurate assumption of constant τ (relaxation time independent of E), which is still widely used in the literature [32].

Using the transport coefficients, one can calculate the electrical conductivity σ , Seebeck coefficient S , and electron thermal conductivity κ_e . They are respectively given by

$$\sigma = q^2 \mathcal{L}_0, \quad (6)$$

$$S = \frac{1}{qT} \frac{\mathcal{L}_1}{\mathcal{L}_0}, \quad (7)$$

and

$$\kappa_e = \frac{1}{T} \left(\mathcal{L}_2 - \frac{(\mathcal{L}_1)^2}{\mathcal{L}_0} \right), \quad (8)$$

From these thermoelectric properties, along with the lattice thermal conductivity κ_{ph} , we can calculate the thermoelectric figure of merit,

$$ZT = \frac{S^2 \sigma}{\kappa_e + \kappa_{\text{ph}}} T. \quad (9)$$

Whenever necessary, especially to simplify some equations, we will use reduced (dimensionless) variables for the energy dispersion $\varepsilon = E/k_B T$, and also for the chemical potential, $\eta = \mu/k_B T$.

The transport coefficients \mathcal{L}_i are generally calculated by considering all bands available within $E = (-\infty, \infty)$. However, in most of materials, thermoelectric properties are dominated by the states near the Fermi energy. In this work, we adopt the two-band model involving a valence band and a conduction band as a minimum requirement to include the bipolar effect (or sign inversion of the Seebeck coefficient), which is always observed in materials having two different types of carriers, i.e., electrons

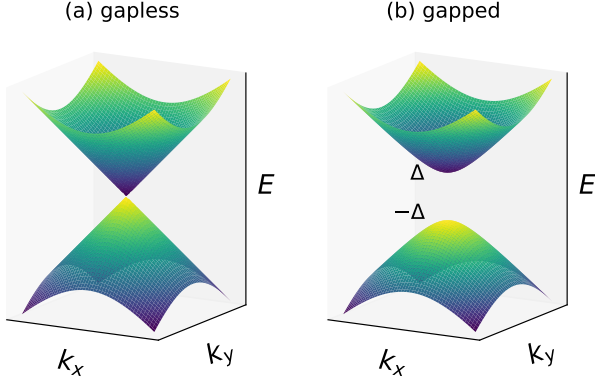


FIG. 1. Schematic two-band energy dispersion for (a) gapless and (b) gapped 2D Dirac materials. Note that the band gap of the gapped Dirac material in this paper is expressed as $E_g = 2\Delta$.

and holes in the conduction and valence bands, respectively. In the two-band model, σ , S , and κ_e can be written as follows [1]:

$$\sigma = \sigma_c + \sigma_v, \quad (10)$$

$$S = \frac{\sigma_c S_c + \sigma_v S_v}{\sigma_c + \sigma_v}, \quad (11)$$

$$\kappa_e = \frac{\sigma_c \sigma_v}{\sigma_c + \sigma_v} (S_c - S_v)^2 + (\kappa_{e,c} + \kappa_{e,v}), \quad (12)$$

where the additional subscript c (v) labels the conduction (valence) band.

Based on Eqs. (10)–(12), the integral \mathcal{L}_i in Eqs. (6)–(8) can be decomposed into $\mathcal{L}_{i,c}$ and $\mathcal{L}_{i,v}$ with the integration over energy intervals $[0, \infty]$ and $[-\infty, 0]$ for the valence and conduction bands, respectively, i.e.,

$$\mathcal{L}_{i,c} = \int_0^\infty \mathcal{T}(E)(E - \mu)^i \left(-\frac{\partial f}{\partial E} \right) dE. \quad (13)$$

and

$$\mathcal{L}_{i,v} = \int_{-\infty}^0 \mathcal{T}(E)(E - \mu)^i \left(-\frac{\partial f}{\partial E} \right) dE. \quad (14)$$

We will show detailed calculations of $\mathcal{L}_{i,c}$ and $\mathcal{L}_{i,v}$ for the gapless 2D Dirac material in Sec. III because it is possible to analytically obtain these integrals for the gapless case. Some variable and unit notations introduced in Sec. III will also be later used in Secs. IV and V when discussing more general cases (both gapped and gapless 2D Dirac materials), in which it is necessary to perform the integration numerically.

III. GAPLESS 2D DIRAC MATERIAL

In the gapless 2D Dirac material, $\Delta = 0$ leads to the TDF independent of E because the group velocity v_g of the massless Dirac electron is constant, $\mathcal{T} = v_g^2 C/2$.

To calculate the integral \mathcal{L}_i , we can separate the energy interval $[0, \infty]$ for the conduction band and $[-\infty, 0]$ for the valence band. For the conduction band, we obtain \mathcal{L}_i as

$$\mathcal{L}_{i,c} = \frac{1}{2} v_g^2 C (k_B T)^i \mathcal{F}_{i,c}(\eta), \quad (15)$$

with

$$\mathcal{F}_{i,c}(\eta) = \int_{-\eta}^\infty \frac{x^i e^x}{(e^x + 1)^2} dx \quad (16)$$

due to the substitution of $x = \varepsilon - \eta$. For $i = 0, 1, 2$, we have:

$$\mathcal{F}_{0,c}(\eta) = \frac{e^\eta}{e^\eta + 1}, \quad (17)$$

$$\mathcal{F}_{1,c}(\eta) = \frac{\eta}{e^\eta + 1} + \ln(1 + e^{-\eta}), \quad (18)$$

$$\mathcal{F}_{2,c}(\eta) = \frac{\pi^2}{3} - \frac{\eta^2}{e^\eta + 1} - 2\eta \ln(1 + e^{-\eta}) + 2\text{Li}_2(-e^{-\eta}), \quad (19)$$

where $\text{Li}_j(z) = \sum_{n=1}^\infty \frac{z^n}{n^j}$ is the polylogarithmic function.

We obtain σ_c , S_c , and $\kappa_{e,c}$ as follows:

$$\begin{aligned} \sigma_c &= q^2 \mathcal{L}_{0,c} \\ &= \frac{1}{2} e^2 v_g^2 C \mathcal{F}_{0,c}(\eta), \end{aligned} \quad (20)$$

$$\begin{aligned} S_c &= \frac{1}{qT} \frac{\mathcal{L}_{1,c}}{\mathcal{L}_{0,c}} \\ &= -\frac{k_B}{e} \frac{\mathcal{F}_{1,c}(\eta)}{\mathcal{F}_{0,c}(\eta)}, \end{aligned} \quad (21)$$

$$\begin{aligned} \kappa_{e,c} &= \frac{1}{T} \left(\mathcal{L}_{2,c} - \frac{(\mathcal{L}_{1,c})^2}{\mathcal{L}_{0,c}} \right) \\ &= \frac{1}{2} v_g^2 C k_B^2 T \left(\mathcal{F}_{2,c}(\eta) - \frac{(\mathcal{F}_{1,c}(\eta))^2}{\mathcal{F}_{0,c}(\eta)} \right), \end{aligned} \quad (22)$$

where $e \approx 1.602 \times 10^{-19}$ C is the elementary charge. For convenience, hereafter we will use the units $S_0 = k_B/e$ (~ 87 $\mu\text{V}/\text{K}$), $\sigma_0 = e^2 v_g^2 C/2$, and $\kappa_0 = v_g^2 C k_B^2 T/2$. We also set the lattice thermal conductivity as an adjustable quantity,

$$\kappa_{\text{ph}} = r_\kappa \kappa_0, \quad (23)$$

where r_κ is a material parameter and may be engineered to maximize the ZT .

Considering only the conduction band, the figure of merit for the gapless 2D Dirac material is given by:

$$\begin{aligned} ZT_c(\eta) &= \frac{S_c^2 \sigma_c}{\kappa_{e,c} + \kappa_{\text{ph}}} T \\ &= \frac{(\mathcal{F}_{1,c}(\eta))^2}{\mathcal{F}_{0,c}(\eta) \mathcal{F}_{2,c}(\eta) - (\mathcal{F}_{1,c}(\eta))^2 + r_\kappa \mathcal{F}_{0,c}}, \end{aligned} \quad (24)$$

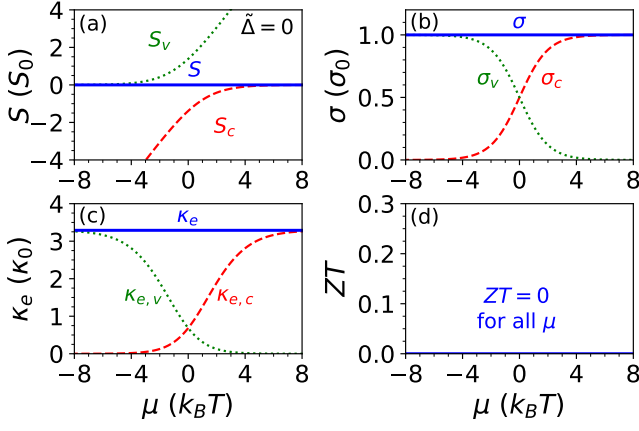


FIG. 2. Thermoelectric properties of gapless 2D Dirac material as a function of chemical potential. (a) Seebeck coefficient in units of $S_0 = k_B/e$. (b) Electrical conductivity in units of $\sigma_0 = e^2 v_g^2 C/2$. (c) Electron thermal conductivity in units of $\kappa_0 = v_g^2 C k_B^2 T$. (d) Dimensionless figure of merit.

Although ZT may have a finite value if we only consider the conduction band as represented by ZT_c , the full expression of the two-band model gives additional terms related to the valence band that will cancel ZT_c and lead to $ZT = 0$ for the gapless 2D Dirac material as shown below.

The TE integral \mathcal{L}_i for the valence band is

$$\mathcal{L}_{i,v} = \frac{1}{2} v_g^2 C (k_B T)^i \mathcal{F}_{i,v}(\eta), \quad (25)$$

with

$$\mathcal{F}_{i,v}(\eta) = \int_{-\infty}^{-\eta} \frac{x^i e^x}{(e^x + 1)^2} dx. \quad (26)$$

For $i = 0, 1, 2$, we have:

$$\mathcal{F}_{0,v}(\eta) = \frac{1}{e^\eta + 1}, \quad (27)$$

$$\mathcal{F}_{1,v}(\eta) = -\frac{\eta}{e^\eta + 1} - \ln(1 + e^{-\eta}), \quad (28)$$

$$\mathcal{F}_{2,v}(\eta) = \frac{\eta^2}{e^\eta + 1} + 2x \ln(1 + e^{-\eta}) - 2\text{Li}_2(-e^{-\eta}). \quad (29)$$

Note that the integrals $\mathcal{F}_{i,c}$ and $\mathcal{F}_{i,v}$ are connected via electron-hole symmetry of the system:

$$\mathcal{F}_{0,c}(\eta) = \mathcal{F}_{0,v}(-\eta) \quad (30a)$$

$$\mathcal{F}_{1,c}(\eta) = -\mathcal{F}_{1,v}(\eta) \quad (30b)$$

$$\mathcal{F}_{2,c}(\eta) = \mathcal{F}_{2,v}(-\eta) \quad (30c)$$

The contribution of the valence band to the thermoelectric quantities σ_v , S_v , and $\kappa_{e,v}$, can be expressed similarly

with that of the conduction band:

$$\sigma_v = \sigma_0 \mathcal{F}_{0,v}(\eta), \quad (31)$$

$$S_v = -S_0 \frac{\mathcal{F}_{1,v}(\eta)}{\mathcal{F}_{0,v}(\eta)}, \quad (32)$$

$$\kappa_{e,v} = \kappa_0 \left(\mathcal{F}_{2,v}(\eta) - \frac{(\mathcal{F}_{1,v}(\eta))^2}{\mathcal{F}_{0,v}(\eta)} \right). \quad (33)$$

Based on the formulas of the two-band model [Eqs. (10)–(12)] and the electron-hole symmetry in the TE integrals [Eq. (30)], it is obvious that the Seebeck coefficient S becomes zero [see Fig. 2(a)], whereas the electrical conductivity σ and electron thermal conductivity κ_e have nonzero (finite) values that are constant for whole η [see Figs. 2(b) and (c)]. As a result, for the gapless 2D Dirac material considered in this work, we have

$$ZT(\eta) = 0. \quad (34)$$

This dramatic result underscores the demerit of electron-hole symmetry for TE performance [see dotted and dashed lines in Figs. 2(a)–(c)]. The competing contribution of electrons and holes persists in the electron-hole symmetric band structures even when the energy gap is introduced. Since the relaxation time is assumed to be inversely proportional to DOS in Eq. (5), the TDF becomes energy-independent and the Seebeck coefficient completely vanishes for all doping levels. We note that such a model fails to describe the region near the Dirac point ($\mu = 0$) as the DOS vanishes. In the realistic situation, the accidentally perfect cancellation may not appear due to the complexity of the scattering mechanism and imperfect electron-hole symmetry. For example, finite Seebeck's coefficient $S \approx 40 - 100 \mu\text{V/K}$ at 300 K was reported for the 2D graphene [33, 34].

The finite Seebeck coefficient is thus expected with dominant contribution coming from the majority carrier (either electron or hole depending on the sign of chemical potential). Although qualitatively less accurate from our theoretical point of view, the constant τ approximation presented in Appendix gives nonzero and finite value of S for the gapless 2D Dirac material. Sharapov and Varlamov in an earlier work also predicted within the constant τ approximation the nonzero value of S in gapless graphene and anomalous growth of S in gapped graphene [35]. To get rid of the poor TE performance due to the electron-hole cancellation, we may apply a magnetic field as a facilitator to break the electron-hole symmetry and thus obtain a larger, nonsaturating Seebeck coefficient [36]. However, applying the magnetic field on the order of several teslas is beyond the current practical capability of the TE industry.

IV. GAPPED 2D DIRAC MATERIAL

Unlike for the gapless 2D Dirac material, the TDF for the gapped 2D Dirac material is now energy-dependent:

$$\mathcal{T}(E) = \frac{Cv_g^2}{2} \left(\frac{E^2 - \Delta^2}{E^2} \right), \quad (35)$$

with the energy intervals $[-\infty, -\Delta]$ and $[\Delta, \infty]$ to be considered in the calculation of the TE integrals. For simplifying the formulation, we define the dimensionless gap,

$$\tilde{\Delta} = \Delta/k_B T \quad (36)$$

The TE integral for the conduction band is

$$\mathcal{L}_{i,c} = \frac{Cv_g^2(k_B T)^i}{2} \left(\mathcal{F}_{i,c}(\eta - \tilde{\Delta}) - \mathcal{G}_{i,c}(\tilde{\Delta}, \eta) \right), \quad (37)$$

with

$$\mathcal{G}_{i,c}(\tilde{\Delta}, \eta) = \int_{\tilde{\Delta}-\eta}^{\infty} \frac{\tilde{\Delta}^2}{(x+\eta)^2} \frac{x^i e^x}{(e^x+1)^2} dx. \quad (38)$$

Similarly, the TE integral for the valence band is

$$\mathcal{L}_{i,v} = \frac{Cv_g^2(k_B T)^i}{2} \left(\mathcal{F}_{i,v}(\eta + \tilde{\Delta}) - \mathcal{G}_{i,v}(\tilde{\Delta}, \eta) \right), \quad (39)$$

with

$$\mathcal{G}_{i,v}(\tilde{\Delta}, \eta) = \int_{-\infty}^{-\tilde{\Delta}-\eta} \frac{\tilde{\Delta}^2}{(x+\eta)^2} \frac{x^i e^x}{(e^x+1)^2} dx. \quad (40)$$

The \mathcal{G}_i integrals for the conduction and valence band contributions are calculated numerically.

Figure 3 depicts the TE properties of the 2D gapped Dirac material. The calculation result of Seebeck coefficient shows finite values whose sign changes across the charge neutrality point, indicating competing contribution of electron and hole, as represented by dotted and dashed lines in Fig. 3(a). The electrical conductivity exhibits a dip in the band gap and saturates to a finite value far away from the gap [Fig. 3(b)]. On the other hand, electron thermal conductivity shows a local maximum at the gap due to the combination of $S_{c,v}$ and $\sigma_{c,v}$ that add each other. The resulting ZT peaks appear slightly above the band edges with a maximum value of about 0.2 for $\tilde{\Delta} = 1$ if no phonon contributes to the thermal conductivity ($r_\kappa = 0$). The ZT peaks monotonically decrease as the phonon contribution to the thermal conductivity increases.

V. OPTIMAL BAND GAP FOR BETTER THERMOELECTRICS

Understanding how band gap alters the TE properties is of importance for designers of TE materials. To see

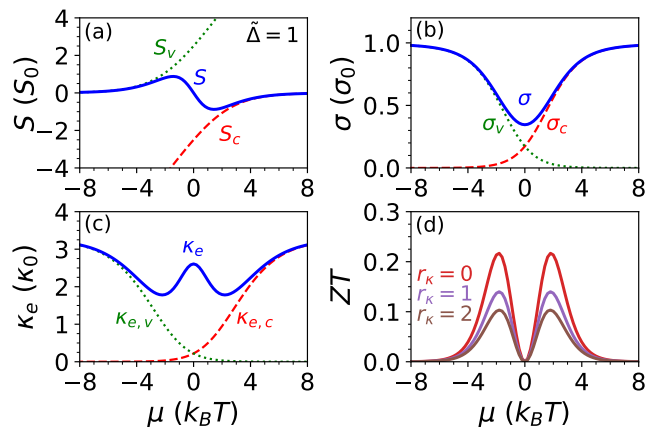


FIG. 3. Thermoelectric properties of a 2D Dirac material with $\tilde{\Delta} = 1$ (equivalently, band gap $E_g = 2k_B T$). (a) Seebeck coefficient in units of $S_0 = k_B/e$. (b) Electrical conductivity in units of $\sigma_0 = e^2 v_g^2 C/2$. (c) Electron thermal conductivity in units of $\kappa_0 = v_g^2 C k_B^2 T$. (d) Dimensionless figure of merit calculated with three different parameters r_κ (representing lattice thermal conductivity).

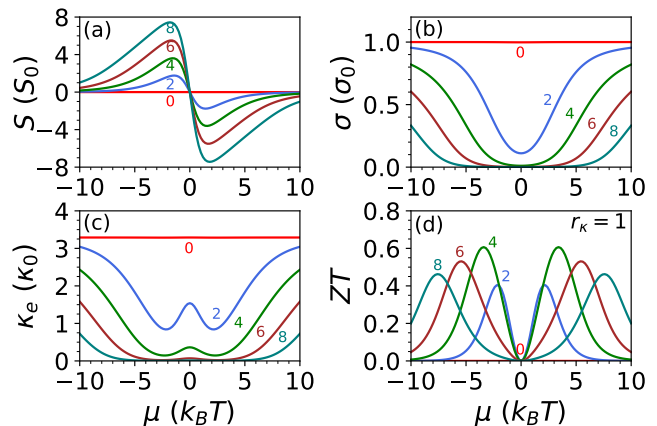


FIG. 4. Thermoelectric properties of 2D Dirac materials calculated for several different gaps, $\tilde{\Delta} = 0, 2, 4, 6, 8$. (a) Seebeck coefficient in units of $S_0 = k_B/e$. (b) Electrical conductivity in units of $\sigma_0 = e^2 v_g^2 C/2$. (c) Electron thermal conductivity in units of $\kappa_0 = v_g^2 C k_B^2 T$. (d) Dimensionless figure of merit ZT with $r_\kappa = 1$. Note that the numbered curves in each figure are used to distinguish $\tilde{\Delta} = 0, 2, 4, 6, 8$, which are equivalent to $E_g/k_B T = 0, 4, 8, 12, 16$.

the evolution of TE properties with respect to the band gap, we show in Fig. 4 the calculation results of S , σ , κ_e , and ZT for $\tilde{\Delta} = 0-8$. As the band gap increases, the Seebeck coefficient monotonically decreases while electrical and electron thermal conductivities increase. Combined action of these interrelated quantities shall give ZT that can be maximized by tuning $\tilde{\Delta}$. For $r_\kappa = 1$, the ZT value reaches maximum near the band edge and becomes largest at $\tilde{\Delta} = 4$ or corresponding band gap $E_g = 8k_B T$ [Fig. 4(d)].

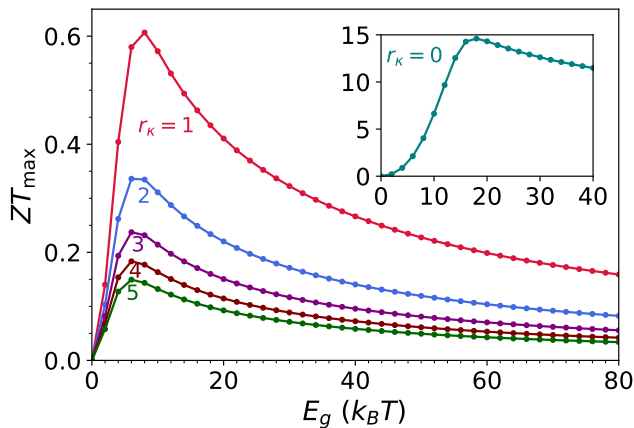


FIG. 5. Maximum ZT values versus band gaps of 2D Dirac materials for several different lattice thermal conductivity parameters r_κ . Inset shows the result for $r_\kappa = 0$ which might be unrealistic but it gives the largest possible ZT .

To find the optimal band gap for the 2D Dirac materials, we can numerically calculate the maximum ZT value scanned through doping levels μ and then plot ZT_{\max} (the maximum ZT found after scanning μ) as a function of E_g and r_κ . The result is shown in Fig. 5. We can see that ZT_{\max} typically peaks at $E_g = 6\text{--}18k_B T$ depending on phonon thermal conductivity coefficient r_κ . By the increase of r_κ , we find that ZT_{\max} tends to be achieved at smaller band gap, saturated at $E_g \sim 6k_B T$. Decreasing phonon thermal conductivity through different methods such as defect engineering, heterostructures and strain is favorable to enhance ZT . For example, the ultralow thermal conductivity denoted by $r_\kappa = 0$ will give the largest possible ZT_{\max} far above unity and it favors larger band gap of about $18k_B T$ as shown in the inset of Fig. 5.

VI. CONCLUSIONS AND PERSPECTIVE

We have shown that optimal band gaps within $6\text{--}18k_B T$ are useful for maximizing ZT in the 2D Dirac materials, where the TE properties were calculated considering the energy-dependent relaxation time $\tau(E)$ inversely proportional to the DOS. This result indicates that the gapless 2D Dirac material is not good for thermoelectrics, but opening a gap of few $k_B T$ is beneficial to enhance its TE properties. The candidates of the gapped 2D Dirac materials that are suitable for TE applications may already possible to fabricate, such as bilayer graphene (with electrically tunable gap) and commensurate graphene-hBN heterostructure [34, 37] whose mini-gap about tens of meV emerges due to inversion symmetry breaking. In particular, the graphene-hBN heterostructure has excellent $S^2\sigma$ [34]. Next, reducing the phonon thermal conductivity to reach ZT that are satisfactory for the TE applications is worth investigating. Our model is also readily extensible for other systems

by using appropriate parameters, so that it may trigger further theoretical works on thermoelectrics. Multiband effect which is not considered in this calculation might enhance ZT and can be incorporated in a straight-forward fashion within linearized Boltzmann transport equation.

ACKNOWLEDGMENTS

E.H. acknowledges research grant from Indonesia Toray Science Foundation. L.P.A., and B.E.G. acknowledge the financial support from Ministry of Research, Technology, and Higher Education of the Republic of Indonesia (Kemendiknas) through PDUPT 2018–2019. N.T.H. acknowledges JSPS KAKENHI Grant No. JP18J10151.

Appendix: Results within constant relaxation time approximation (CRTA)

Here we present the calculation of TE properties of 2D Dirac materials within the constant relaxation time approximation (CRTA). The results within this approximation overestimate the value of S and σ in comparison to those given in the main text. As a result, the gapless 2D Dirac material will have finite (nonzero) S , unlike what we have shown in the main text.

In the CRTA, the transport distribution function for the 2D Dirac materials is given by

$$\mathcal{T}(E) = \tau_0 \left[\frac{v_g^2}{2} \left(\frac{E^2 - \Delta^2}{E^2} \right) \right] \mathcal{D}(E), \quad (\text{A.1})$$

where τ_0 is the relaxation time constant. The density of states is defined by

$$\mathcal{D}(E) = \frac{g|E|}{2\pi L(\hbar v_g)^2} \Theta(|E| - |\Delta|), \quad (\text{A.2})$$

where g is degeneracies, L is the confinement length, and $\Theta(x)$ is the Heaviside step function, i.e., $\Theta(x) = 1$ if $x > 0$ and $\Theta(x) = 0$ otherwise.

After some algebra [32], we can obtain the TE integral for the conduction band of the 2D Dirac material within the CRTA as

$$\begin{aligned} \mathcal{L}_{i,c} = & \frac{g\tau_0}{4\pi\hbar^2 L} (k_B T)^{i+1} \left[\mathcal{F}_{i+1,c}(\eta - \tilde{\Delta}) \right. \\ & \left. + \eta \mathcal{F}_{i,c}(\eta - \tilde{\Delta}) - \tilde{\mathcal{G}}_{i,c}(\tilde{\Delta}, \eta) \right], \end{aligned} \quad (\text{A.3})$$

with

$$\tilde{\mathcal{G}}_{i,c}(\tilde{\Delta}, \eta) = \int_{\tilde{\Delta}-\eta}^{\infty} \frac{\tilde{\Delta}^2}{(x+\eta)} \frac{x^i e^x}{(e^x+1)^2} dx. \quad (\text{A.4})$$

Similarly, the TE integral for the valence band is

$$\begin{aligned} \mathcal{L}_{i,v} = & - \frac{g\tau_0}{4\pi\hbar^2 L} (k_B T)^{i+1} \left[\mathcal{F}_{i+1,v}(\eta + \tilde{\Delta}) \right. \\ & \left. + \eta \mathcal{F}_{i,v}(\eta + \tilde{\Delta}) - \tilde{\mathcal{G}}_{i,v}(\tilde{\Delta}, \eta) \right], \end{aligned} \quad (\text{A.5})$$

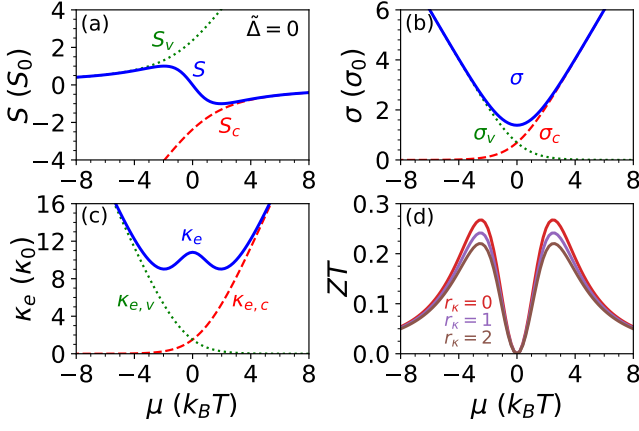


FIG. 6. Thermoelectric properties of gapless 2D Dirac material as a function of chemical potential within the CRTA. (a) Seebeck coefficient in units of $S_0 = k_B/e$. (b) Electrical conductivity in units of $\sigma_0 = g\tau_0 e^2 k_B T / (4\pi\hbar^2 L)$. (c) Electron thermal conductivity in units of $\kappa_0 = g\tau_0 k_B^3 T^2 / (4\pi\hbar^2 L)$. (d) Dimensionless figure of merit.

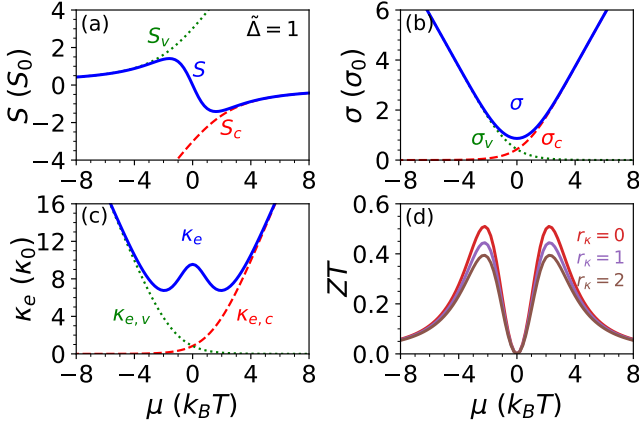


FIG. 7. Thermoelectric properties of a 2D Dirac material within the CRTA for $\tilde{\Delta} = 1$ (equivalently, band gap $E_g = 2k_B T$). (a) Seebeck coefficient in units of $S_0 = k_B/e$. (b) Electrical conductivity in units of $\sigma_0 = g\tau_0 e^2 k_B T / (4\pi\hbar^2 L)$. (c) Electron thermal conductivity in units of $\kappa_0 = g\tau_0 k_B^3 T^2 / (4\pi\hbar^2 L)$. (d) Dimensionless figure of merit calculated with three different parameters r_κ (representing lattice thermal conductivity).

with

$$\tilde{G}_{i,v}(\tilde{\Delta}, \eta) = \int_{-\infty}^{-\tilde{\Delta}-\eta} \frac{\tilde{\Delta}^2}{(x+\eta)} \frac{x^i e^x}{(e^x+1)^2} dx. \quad (\text{A.6})$$

The remaining calculation procedure to obtain the TE properties is the same as in the main text. Due to the complexity of \mathcal{L}_i , the integration in this case should also be performed numerically. Note that, in addition to \mathcal{F}_0 , \mathcal{F}_1 , and \mathcal{F}_2 , we have to employ \mathcal{F}_3 according to the recursive relation of \mathcal{L}_i in Eqs. (A.3) and (A.5). The formulas for $\mathcal{F}_{3,c}$ and $\mathcal{F}_{3,v}$ are

$$\mathcal{F}_{3,c}(\eta) = \eta^2 \left[\frac{\eta}{1+e^\eta} + 3 \ln(1+e^{-\eta}) \right] - 6\eta \text{Li}_2(-e^{-\eta}) - 6\text{Li}_3(-e^{-\eta}) \quad (\text{A.7})$$

and

$$\mathcal{F}_{3,v}(\eta) = \eta^2 \left[-\frac{\eta}{1+e^\eta} - 3 \ln(1+e^{-\eta}) \right] + 6\eta \text{Li}_2(-e^{-\eta}) + 6\text{Li}_3(-e^{-\eta}) \quad (\text{A.8})$$

respectively.

Figures 6 and 7 show the results of TE properties of the 2D Dirac materials within the CRTA by using the same parameters as in Figs. 2 (gapless, $\tilde{\Delta} = 0$) and 3 (gapped, $\tilde{\Delta} = 1$). Within the CRTA, we can see that all the TE properties are overestimated. The most notable feature is the nonzero S for the gapless 2D Dirac material [Fig. 6(a)], which leads to the finite ZT [Fig. 6(d)] for different r_κ values. Similarly, ZT for the gapped 2D Dirac material within the CRTA is also larger than that shown in the main text.

- [1] H. J. Goldsmid, *Introduction to Thermoelectricity* (Springer-Verlag, Berlin Heidelberg, 2010).
- [2] J. P. Heremans, M. S. Dresselhaus, L. E. Bell, and D. T. Morelli, “When thermoelectrics reached the nanoscale,” *Nat. Nanotechnol.* **8**, 471–473 (2013).
- [3] Y. Pei, X. Shi, A. LaLonde, H. Wang, L. Chen, and G. J. Snyder, “Convergence of electronic bands for high performance bulk thermoelectrics,” *Nature* **473**, 66–69 (2011).
- [4] K. Biswas, J. He, I. D. Blum, C. I. Wu, T. P. Hogan, D. N. Seidman, V. P. Dravid, and M. G. Kanatzidis,

- “High-performance bulk thermoelectrics with all-scale hierarchical architectures,” *Nature* **489**, 414 (2012).
- [5] L. D. Hicks and M. S. Dresselhaus, “Effect of quantum-well structures on the thermoelectric figure of merit,” *Phys. Rev. B* **47**, 12727 (1993).
- [6] N. T. Hung, E. H. Hasdeo, A. R. T. Nugraha, M. S. Dresselhaus, and R. Saito, “Quantum effects in the thermoelectric power factor of low-dimensional semiconductors,” *Phys. Rev. Lett.* **117**, 036602 (2016).
- [7] A. Majumdar, “Thermoelectricity in semiconductor nanostructures,” *Science* **303**, 777 (2004).

- [8] C. B. Vining, “An inconvenient truth about thermoelectrics,” *Nat. Mater.* **8**, 83 (2009).
- [9] G. D. Mahan and J. O. Sofo, “The best thermoelectric,” *Proc. Natl. Acad. Sci. U.S.A.* **93**, 7436 (1996).
- [10] J. Zhou, R. Yang, G. Chen, and M. S. Dresselhaus, “Optimal bandwidth for high efficiency thermoelectrics,” *Phys. Rev. Lett.* **107**, 226601 (2011).
- [11] J. O. Sofo and G. D. Mahan, “Optimum band gap of a thermoelectric material,” *Phys. Rev. B* **49**, 4565 (1994).
- [12] L. D. Hicks and M. S. Dresselhaus, “Thermoelectric figure of merit of a one-dimensional conductor,” *Phys. Rev. B* **47**, 16631 (1993).
- [13] L. D. Hicks, T. C. Harman, X. Sun, and M. S. Dresselhaus, “Experimental study of the effect of quantum-well structures on the thermoelectric figure of merit,” *Phys. Rev. B* **53**, R10493 (1996).
- [14] M. S. Dresselhaus, G. Chen, M. Y. Tang, R. G. Yang, H. Lee, D. Z. Wang, Z. F. Ren, J. P. Fleurial, and P. Gogna, “New directions for low-dimensional thermoelectric materials,” *Adv. Mater.* **19**, 1043 (2007).
- [15] G. Zhang and Y.-W. Zhang, “Thermoelectric properties of two-dimensional transition metal dichalcogenides,” *J. Mater. Chem. C* **5**, 7684 (2017).
- [16] K. Hippalgaonkar, Y. Wang, Y. Ye, D. Y. Qiu, H. Zhu, Y. Wang, J. Moore, S. G. Louie, and X. Zhang, “High thermoelectric power factor in two-dimensional crystals of MoS₂,” *Phys. Rev. B* **95**, 115407 (2017).
- [17] M. J. Lee, J. H. Ahn, J. H. Sung, H. Heo, S. G. Jeon, W. Lee, J. Y. Song, K.-H. Hong, B. Choi, S. H. Lee, and M. H. Jo, “Thermoelectric materials by using two-dimensional materials with negative correlation between electrical and thermal conductivity,” *Nat. Commun.* **7**, 12011 (2016).
- [18] D. Wickramaratne, F. Zahid, and R. K. Lake, “Electronic and thermoelectric properties of van der Waals materials with ring-shaped valence bands,” *J. Appl. Phys.* **118**, 075101 (2015).
- [19] K. Yang, S. Cahangirov, A. Cantarero, A. Rubio, and R. D’Agosta, “Thermoelectric properties of atomically thin silicene and germanene nanostructures,” *Phys. Rev. B* **89**, 125403 (2014).
- [20] Z. Ni, Q. Liu, K. Tang, J. Zheng, J. Zhou, R. Qin, Z. Gao, D. Yu, and J. Lu, “Tunable bandgap in silicene and germanene,” *Nano Lett.* **12**, 113 (2012).
- [21] G. Tan, L.-D. Zhao, F. Shi, J. W. Doak, S.-H. Lo, H. Sun, C. Wolverton, V. P. Dravid, C. Uher, and M. G. Kanatzidis, “High thermoelectric performance of p-type SnTe via a synergistic band engineering and nanostructuring approach,” *J. Am. Chem. Soc.* **136**, 7006 (2014).
- [22] E. Zaminpayma and P. Nayebi, “Band gap engineering in silicene: A theoretical study of density functional tight-binding theory,” *Phys. E* **84**, 555 (2016).
- [23] A. Castellanos-Gomez, “Why all the fuss about 2D semiconductors?” *Nat. Photonics* **10**, 202 (2016).
- [24] L. D. Zhao, S. H. Lo, Y. Zhang, H. Sun, G. Tan, C. Uher, C. Wolverton, V. P. Dravid, and M. G. Kanatzidis, “Ultralow thermal conductivity and high thermoelectric figure of merit in SnSe crystals,” *Nature* **508**, 374 (2014).
- [25] Z. M. Gibbs, H. S. Kim, H. Wang, and G. J. Snyder, “Band gap estimation from temperature dependent seebeck measurement-deviations from the $2e|S|_{\max}T_{\max}$ relation,” *Appl. Phys. Lett.* **106**, 022112 (2015).
- [26] Y. Anno, Y. Imakita, K. Takei, S. Akita, and T. Arie, “Enhancement of graphene thermoelectric performance through defect engineering,” *2D Mat.* **4**, 025019 (2017).
- [27] D. Qin, X. J. Ge, G. Q. Ding, G. Y. Gao, and J. T. Lu, “Strain-induced thermoelectric performance enhancement of monolayer ZrSe₂,” *RSC Adv.* **7**, 47243 (2017).
- [28] S. I. Kim, K. H. Lee, H. A. Mun, H. S. Kim, S. W. Hwang, J. W. Roh, D. J. Yang, W. H. Shin, X. S. Li, Y. H. Lee, G. J. Snyder, and S. W. Kim, “Dense dislocation arrays embedded in grain boundaries for high-performance bulk thermoelectrics,” *Science* **348**, 109–114 (2015).
- [29] N. T. Hung, A. R. T. Nugraha, and R. Saito, “Two-dimensional InSe as a potential thermoelectric material,” *Appl. Phys. Lett.* **111**, 092107 (2017).
- [30] N. T. Hung, A. R. T. Nugraha, and R. Saito, “Universal curve of optimum thermoelectric figures of merit for bulk and low-dimensional semiconductors,” *Phys. Rev. Appl.* **9**, 024019 (2018).
- [31] J. Zhou, R. Yang, G. Chen, and M. S. Dresselhaus, “Optimal bandwidth for high efficiency thermoelectrics,” *Phys. Rev. Lett.* **107**, 226601 (2011).
- [32] Detailed notes, derivations, and codes for all results in this paper (both in the main text and Appendix) are available at <http://github.com/artnugraha/DiracTE>.
- [33] F. Ghahari, H. Y. Xie, T. Taniguchi, K. Watanabe, M. S. Foster, and P. Kim, “Enhanced thermoelectric power in graphene: Violation of the Mott relation by inelastic scattering,” *Phys. Rev. Lett.* **116**, 136802 (2016).
- [34] J. Duan, X. Wang, X. Lai, G. Li, K. Watanabe, T. Taniguchi, M. Zabarjadi, and E. Y. Andrei, “High thermoelectric power factor in graphene/hBN devices,” *Proc. Natl. Acad. Sci. USA* **113**, 14272 (2016).
- [35] S. G. Sharapov and A. A. Varlamov, “Anomalous growth of thermoelectric power in gapped graphene,” *Phys. Rev. B* **86**, 035430 (2012).
- [36] B. Skinner and L. Fu, “Large, nonsaturating thermopower in a quantizing magnetic field,” *Sci. Adv.* **4**, eaat2621 (2018).
- [37] B. Hunt, J. D. Sanchez-Yamagishi, A. F. Young, M. Yankowitz, B. J. LeRoy, K. Watanabe, T. Taniguchi, P. Moon, M. Koshino, P. Jarillo-Herrero, and R. C. Ashoori, “Massive Dirac fermions and Hofstadter butterfly in a van der Waals heterostructure,” *Science* **340**, 1427 (2013).